

# Lattice gauge theory studies of the gluon propagator

D. B. Leinweber, J. I. Skullerud,<sup>a</sup> and A. G. Williams  
*CSSM and Department of Physics and Mathematical Physics,*  
*The University of Adelaide, SA 5005, Australia*  
<http://www.physics.adelaide.edu.au/theory/>

The gluon propagator in Landau gauge is calculated in quenched QCD on a large ( $32^3 \times 64$ ) lattice at  $\beta = 6.0$ . In order to assess finite volume and finite lattice spacing artefacts, we also calculate the propagator on a smaller volume for two different values of the lattice spacing. New structure seen in the infrared region survives conservative cuts to the lattice data, and serves to exclude a number of models that have appeared in the literature.

## 1 Introduction

The infrared behaviour of the gluon propagator is important for an understanding of confinement. Previous conjectures range from a strong divergence<sup>1,2</sup> to a propagator that vanishes in the infrared<sup>3,4</sup>.

Lattice QCD should in principle be able to resolve this issue by first-principles, model-independent calculations. However, lattice studies have been inconclusive up to now,<sup>5,6</sup> since they have not been able to access sufficiently low momenta. The lower limit of the available momenta on the lattice is given by  $q_{\min} = 2\pi/L$ , where  $L$  is the length of the lattice. Here we will report results using a lattice with a length of 3.3 fm in the spatial directions and 6.7 fm in the time direction. This gives us access to momenta as small as 400 MeV.

## 2 Lattice formalism

The gluon field  $A_\mu$  can be extracted from the link variables  $U_\mu(x)$  using

$$U_\mu(x) = e^{ig_0 a A_\mu(x + \hat{\mu}/2)} + \mathcal{O}(a^3). \quad (1)$$

Inverting and Fourier transforming this, we obtain

$$\begin{aligned} A_\mu(\hat{q}) &\equiv \sum_x e^{-i\hat{q}\cdot(x+\hat{\mu}/2)} A_\mu(x + \hat{\mu}/2) \\ &= \frac{e^{-i\hat{q}_\mu a/2}}{2ig_0 a} \left[ (U_\mu(\hat{q}) - U_\mu^\dagger(-\hat{q})) - \frac{1}{3} \text{Tr} (U_\mu(\hat{q}) - U_\mu^\dagger(-\hat{q})) \right], \quad (2) \end{aligned}$$

---

<sup>a</sup>UKQCD Collaboration

where  $U_\mu(\hat{q}) \equiv \sum_x e^{-i\hat{q}x} U_\mu(x)$  and  $A_\mu(\hat{q}) \equiv t^a A_\mu^a(\hat{q})$ . The available momentum values  $\hat{q}$  are given by

$$\hat{q}_\mu = 2\pi n_\mu / (aN_\mu), \quad n_\mu = 0, \dots, N_\mu - 1 \quad (3)$$

where  $N_\mu$  is the number of points in the  $\mu$  direction. The gluon propagator  $D_{\mu\nu}^{ab}(\hat{q})$  is defined as

$$D_{\mu\nu}^{ab}(\hat{q}) = \langle A_\mu^a(\hat{q}) A_\nu^b(-\hat{q}) \rangle / V. \quad (4)$$

In the continuum Landau gauge, the propagator has the structure

$$D_{\mu\nu}^{ab}(q) = \delta^{ab} (\delta_{\mu\nu} - \frac{q_\mu q_\nu}{q^2}) D(q^2). \quad (5)$$

At tree level,  $D(q^2)$  will have the form

$$D^{(0)}(q^2) = 1/q^2. \quad (6)$$

On the lattice, this becomes

$$D^{(0)}(\hat{q}) = 1 / \sum_\mu \left( \frac{2}{a} \sin \frac{\hat{q}_\mu a}{2} \right). \quad (7)$$

Since QCD is asymptotically free, we expect that up to logarithmic corrections,  $q^2 D(q^2) \rightarrow 1$  in the ultraviolet. Hence we define the new momentum variable  $q$  by

$$q_\mu \equiv \frac{2}{a} \sin \frac{\hat{q}_\mu a}{2}, \quad (8)$$

and work with this throughout.

The (bare) lattice gluon propagator is related to the renormalised continuum propagator  $D_R(q; \mu)$  via

$$D^L(qa) = Z_3(\mu, a) D_R(q; \mu). \quad (9)$$

The renormalisation constant  $Z_3(\mu, a)$  can be found by imposing a momentum subtraction renormalisation condition  $D_R(q)|_{q^2=\mu^2} = \frac{1}{\mu^2}$ .

The asymptotic behaviour of the renormalised gluon propagator in the continuum is given to one-loop level by

$$D_R(q) \equiv D_{\text{bare}}(q) / Z_3 = \frac{1}{q^2} \left( \frac{1}{2} \ln(q^2 / \Lambda^2) \right)^{-d_D} \quad (10)$$

with

$$d_D = \frac{39 - \xi - 4N_f}{4(33 - 2N_f)} = \frac{13}{44}, \quad (11)$$

where both the gauge parameter  $\xi$  and the number of fermion flavours  $N_f$  are zero in this calculation.

Name	$\beta$	$a_{\text{st}}^{-1}$ (GeV)	Volume	$N_{\text{conf}}$	$a\hat{q}_{\text{Max}}$	$ \partial_{\mu}A_{\mu} $
Small	6.0	1.885	$16^3 \times 48$	125	$2\pi/4$	$< 10^{-6}$
Large	6.0	1.885	$32^3 \times 64$	75	$2\pi/4$	$< 10^{-6}$
Fine	6.2	2.63	$24^3 \times 48$	223	$2\pi/4$	$< 10^{-6}$

Table 1: Simulation parameters

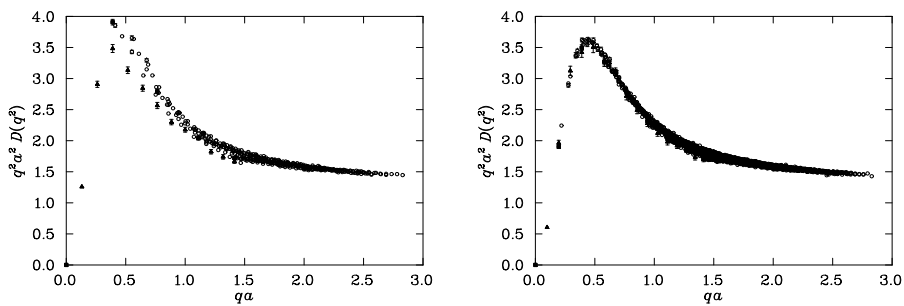


Figure 1: Componentwise data, for the small lattice (left) and the large lattice (right). The filled triangles denote momenta directed along the time axis, while the filled squares denote momenta directed along one of the spatial axes.

### 3 Simulation Parameters, Finite Size Effects and Anisotropies

We have analysed three lattices, with different values for the volume and lattice spacing. The details are given in table 1. In the following, we are particularly interested in the deviation of the gluon propagator from the tree level form. We will therefore factor out the tree level behaviour and plot  $q^2 D(q^2)$  rather than  $D(q^2)$  itself.

Fig. 1 shows the gluon propagator as a function of  $qa$  for the small and large lattices, with momenta in different directions plotted separately. For low momentum values on the small lattice, there are large discrepancies due to finite size effects between points representing momenta along the time axis and those representing momenta along the spatial axes. These discrepancies are absent from the data from the large lattice, indicating that finite size effects here are under control.

However, at higher momenta, there are anisotropies which remain for the large lattice data, and which are of approximately the same magnitude for the two lattices. In order to eliminate these anisotropies, which arise from finite lattice spacing errors, we select momenta lying within a cylinder of radius  $\Delta\hat{q}a = 2 \times 2\pi/32$  along the 4-dimensional diagonals.<sup>9</sup>

#### 4 Scaling behaviour

Since the renormalised propagator  $D_R(q; \mu)$  is independent of the lattice spacing, we can use (9) to derive a simple,  $q$ -independent expression for the ratio of the unrenormalised lattice gluon propagators at the same value of  $q$ :

$$\frac{D_c(qa_c)}{D_f(qa_f)} = \frac{Z_3(\mu, a_c)D_R(q; \mu)/a_c^2}{Z_3(\mu, a_f)D_R(q; \mu)/a_f^2} = \frac{Z_c a_f^2}{Z_f a_c^2} \quad (12)$$

where the subscript  $f$  denotes the finer lattice ( $\beta = 6.2$  in this study) and the subscript  $c$  denotes the coarser lattice ( $\beta = 6.0$ ). We can use this relation to study directly the scaling properties of the lattice gluon propagator by matching the data for the two values of  $\beta$ . This matching can be performed by adjusting the values for the ratios  $R_Z = Z_f/Z_c$  and  $R_a = a_f/a_c$  until the two sets of data lie on the same curve.

We have implemented this by making a linear interpolation of the logarithm of the data plotted against the logarithm of the momentum for both data sets. In this way the scaling of the momentum is accounted for by shifting the fine lattice data to the right by an amount  $\Delta_a$  as follows

$$\ln D_c(\ln(qa_c)) = \ln D_f(\ln(qa_c) - \Delta_a) + \Delta_Z \quad (13)$$

Here  $\Delta_Z$  is the amount by which the fine lattice data must be shifted up to provide the optimal overlap between the two data sets. The matching of the two data sets has been performed for values of  $\Delta_a$  separated by a step size of 0.001.  $\Delta_Z$  is determined for each value of  $\Delta_a$  considered, and the optimal combination of shifts is identified by searching for the global minimum of the  $\chi^2/\text{dof}$ . The ratios  $R_a$  and  $R_Z$  are related to  $\Delta_a$  and  $\Delta_Z$  by

$$R_a = e^{-\Delta_a}, \quad R_Z = R_a^2 e^{-\Delta_Z}. \quad (14)$$

Fig. 2 shows the data for both lattice spacings as a function of  $qa$  before shifting. In the leftmost plot of fig. 3 we present the result of the matching using  $\hat{q}$  as the momentum variable. The minimum value for  $\chi^2/\text{dof}$  of about 1.7 is obtained for  $R_a \sim 0.815$ . This value for  $R_a$  is considerably higher than the value of  $0.716 \pm 0.040$  obtained from an analysis of the static quark potential in <sup>8</sup>. From this discrepancy, as well as the relatively high value for  $\chi^2/\text{dof}$ , we may conclude that the gluon propagator, taken as a function of  $\hat{q}$ , does not exhibit scaling behaviour for the values of  $\beta$  considered here.

The rightmost plot of fig. 3 shows the result of the matching using  $q$  of (8) as the momentum variable. We can see immediately that this gives much more satisfactory values both for  $\chi^2/\text{dof}$  and for  $R_a$ . The minimum value for

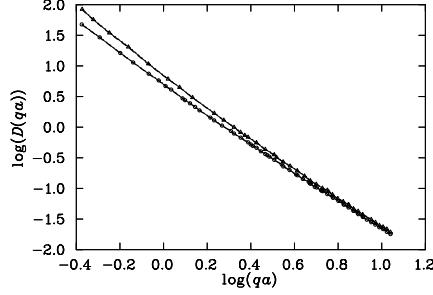


Figure 2: The dimensionless, unrenormalised gluon propagator as a function of  $\ln(qa)$  for the two values of  $\beta$ . The triangles denote the data for the small lattice at  $\beta = 6.0$ , while the circles denote the data for  $\beta = 6.2$ .

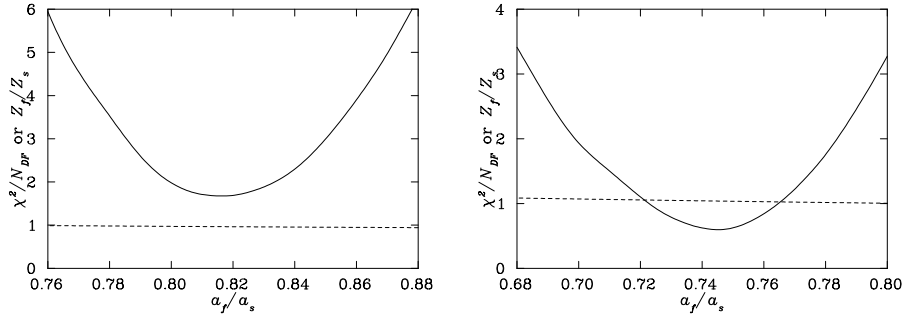


Figure 3:  $\chi^2$  per degree of freedom as a function of the ratio of lattice spacings for matching the small and fine lattice data according to (13), using  $\hat{q}$  (left) and  $q$  (right) as the momentum variable. The dashed line indicates the ratio  $R_Z$  of the renormalisation constants.

$\chi^2/\text{dof}$  of 0.6 is obtained for  $R_a = 0.745$ . Taking a confidence interval where  $\chi^2/\text{dof} < \chi_{min}^2 + 1$  gives us an estimate of  $R_a = 0.745^{+32}_{-37}$ , which is fully compatible with the value<sup>8</sup> of  $0.716 \pm 0.040$ . The corresponding estimate for the ratio of the renormalisation constants is  $R_Z = 1.038^{+26}_{-21}$ .

## 5 Model Fits

We have demonstrated scaling in our lattice data over the entire range of  $q^2$  considered, and will now proceed with model fits. The following functional forms have been considered:

$$D(q^2) = \frac{Zq^2}{q^4 + M^4} \left( \frac{1}{2} \ln \frac{q^2 + M^2}{M^2} \right)^{-d_D} \quad (\text{Gribov}^3) (15)$$

$$D(q^2) = Z \frac{q^2}{q^4 + 2A^2 q^2 + M^4} \left( \frac{1}{2} \ln \frac{q^2 + M^2}{M^2} \right)^{-d_D} \quad (\text{Stingl}^4) (16)$$

$$D(q^2) = \frac{Z}{(q^2)^{1+\alpha} + M^2} \quad (\text{Marenzoni } et al^6) (17)$$

$$D(q^2) = Z \left[ (q^2 + M^2(q^2)) \ln \frac{q^2 + 4M^2(q^2)}{\Lambda^2} \right]^{-1} \quad (\text{Cornwall}^7) (18)$$

$$\text{where } M(q^2) = M \left\{ \ln \frac{q^2 + 4M^2}{\Lambda^2} / \ln \frac{4M^2}{\Lambda^2} \right\}^{-6/11}$$

$$D(q^2) = Z \left( \frac{A}{(q^2 + M_{\text{IR}}^2)^{1+\alpha}} + \frac{1}{q^2 + M_{\text{UV}}^2} \left( \frac{1}{2} \ln \frac{q^2 + M_{\text{UV}}^2}{M_{\text{UV}}^2} \right)^{-d_D} \right) \quad (19)$$

$$D(q^2) = Z \left( \frac{A}{(q^2)^{1+\alpha} + (M_{\text{IR}}^2)^{1+\alpha}} + \frac{1}{q^2 + M_{\text{UV}}^2} \left( \frac{1}{2} \ln \frac{q^2 + M_{\text{UV}}^2}{M_{\text{UV}}^2} \right)^{-d_D} \right) \quad (20)$$

$$D(q^2) = Z \left( A e^{-(q^2/M_{\text{IR}}^2)^\alpha} + \frac{1}{q^2 + M_{\text{UV}}^2} \left( \frac{1}{2} \ln \frac{q^2 + M_{\text{UV}}^2}{M_{\text{UV}}^2} \right)^{-d_D} \right) \quad (21)$$

We have also considered<sup>10</sup> special cases of the three forms (19)–(21), with  $M_{\text{IR}} = M_{\text{UV}}$  or with specific values for the exponent  $\alpha$ . Equations (15) and (16) are modified in order to exhibit the asymptotic behaviour of (10). Models (19) and (20) are constructed as generalisations of (17) with the correct dimension and asymptotic behaviour.

All models were fitted to the large lattice data using the cylindrical cut. The lowest momentum value was excluded, as the volume dependence of this point could not be assessed. In order to balance the sensitivity of the fit between the high- and low-momentum region, nearby data points within  $\Delta(qa) < 0.05$  were averaged.

$\chi^2$  per degree of freedom and parameter values for fits to all these models are shown in table 2. It is clear that model (20) accounts for the data better than any of the other models. The best fit to this model is illustrated in fig. 4.

## 6 Discussion and Outlook

We have evaluated the gluon propagator on an asymmetric lattice with a large physical volume. By studying the anisotropies in the data, and comparing the data with those from a smaller lattice, we have been able to conclude that finite size effects are under control on the large lattice.

A clear turnover in the behaviour of  $q^2 D(q^2)$  has been observed at  $q \sim 1 \text{ GeV}$ , indicating that the gluon propagator diverges less rapidly than  $1/q^2$  in the infrared, and may be infrared finite or vanishing.

The data are consistent with a functional form  $D(q^2) = D_{\text{IR}} + D_{\text{UV}}$ , where

$$D_{\text{IR}} = \frac{1}{2} \frac{1}{q^4 + M^4}, \quad (22)$$

Model	$\chi^2/\text{dof}$	$Z$	$A$	$M_{\text{IR}}$	$M_{\text{UV}}$ or $\Lambda$	$\alpha$
15	1972	$2.19^{+31}_{-15}$		$0.23^{+14}_{-1}$		
16	1998	2.2	0	0.23		
17	163	$2.41^{+0}_{-12}$		$0.14^{+4}_{-14}$		$0.29^{+6}_{-2}$
18	50.3	$6.5^{+7}_{-9}$		$0.24^{+3}_{-16}$	$0.27^{+7}_{-7}$	
19	2.96	$1.54^{+10}_{-20}$	$1.24^{+21}_{-21}$	$0.46^{+2}_{-14}$	$0.96^{+47}_{-17}$	$1.31^{+16}_{-43}$
19; $M_{\text{IR}} = M_{\text{UV}}$	3.73	$1.71^{+9}_{-0}$	$0.84^{+0}_{-29}$	$0.48^{+2}_{-17}$		$1.52^{+12}_{-37}$
20	1.57	$1.78^{+45}_{-20}$	$0.49^{+17}_{-6}$	$0.43^{+5}_{-1}$	$0.20^{+37}_{-19}$	$0.95^{+7}_{-5}$
20; $M_{\text{IR}} = M_{\text{UV}}$	4.00	$1.62^{+3}_{-4}$	$0.58^{+5}_{-1}$	$0.40^{+9}_{-2}$		$0.92^{+17}_{-1}$
21	47	$2.09^{+30}_{-12}$	$29^{+166}_{-2}$	$0.22^{+0}_{-16}$	$0.14^{+11}_{-10}$	$0.49^{+0}_{-16}$

Table 2: Parameter values for fits to models (15)–(21). The values quoted are for fits to the entire set of data. The errors denote the uncertainties in the last digit(s) of the parameter values which result from varying the fitting range. The fitting ranges considered when evaluating the uncertainties are those with a minimum of 40 points included and with the minimum value for  $qa$  no larger than 1.03 (point number 40).

$M \sim 1$  GeV, and  $D_{\text{UV}}$  is the asymptotic form given by (10). A more detailed analysis<sup>10</sup> of the asymptotic behaviour reveals that the one-loop formula (10) remains insufficient at  $q^2 = 50\text{GeV}^2$ .

Issues for future study include the effect of Gribov copies and of dynamical fermions. We also hope to use improved actions to perform realistic simulations at larger lattice spacings. This would enable us to evaluate the gluon propagator on larger physical volumes, giving access to lower momentum values.

## Acknowledgments

The numerical work was mainly performed on a Cray T3D at EPCC, University of Edinburgh, using UKQCD Collaboration time under PPARC Grant GR/K41663. Financial support from the Australian Research Council is gratefully acknowledged. We thank Claudio Parrinello for stimulating discussions.

1. S. Mandelstam, *Phys. Rev.* **D 20**, 3223 (1979)
2. N. Brown and M.R. Pennington, *Phys. Rev.* **D 39**, 2723 (1989)
3. V.N. Gribov, *Nucl. Phys.* **B 139**, 19 (1978); D. Zwanziger, *Nucl. Phys.* **B 378**, 525 (1992)
4. M. Stingl, *Phys. Rev.* **D 34**, 3863 (1986); *Phys. Rev.* **D 36**, 651 (1987)
5. C. Bernard, C. Parrinello, A. Soni, *Phys. Rev.* **D49**, 1585 (1994)

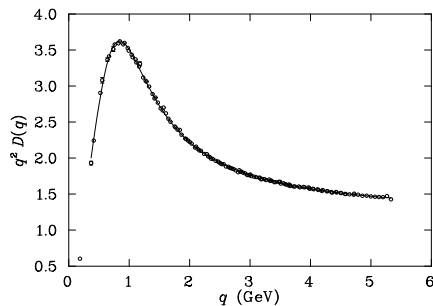


Figure 4: The gluon propagator multiplied by  $q^2$ , with nearby points averaged. The line illustrates our best fit to the form defined in (20). The fit is performed over all points shown, excluding the one at the lowest momentum value, which may be sensitive to the finite volume of the lattice. The scale is taken from the string tension<sup>8</sup>.

6. P. Marenzoni, G. Martinelli, N. Stella, *Nucl. Phys.* **B 455**, 339 (1995);  
P. Marenzoni *et al*, *Phys. Lett.* **B 318**, 511 (1993)
7. J. Cornwall, *Phys. Rev.* **D 26**, 1453 (1982)
8. G.S. Bali and K. Schilling, *Phys. Rev.* **D 47**, 661 (1993)
9. D.B. Leinweber, C. Parrinello, J.I. Skullerud, A.G. Williams, *Phys. Rev.* **D 58**, 031501 (1998)
10. D.B. Leinweber, C. Parrinello, J.I. Skullerud, A.G. Williams, in preparation.